

Activities of MnO in CaO-SiO₂-Al₂O₃-MnO (<10 Pct)-Fe₂O (<3 Pct) Slags Saturated with Liquid Iron

HIROKI OHTA and HIDEAKI SUITO

Activity coefficients of MnO and Fe₂O in CaO-SiO₂-Al₂O₃-MnO (<10 mass pct)-Fe₂O (<3 mass pct) slags were determined at 1873 K in an Al₂O₃ or CaO crucible by using the reported values for the activities of Al₂O₃ and SiO₂ or the analyzed contents of oxygen. The activity coefficients of MnO and Fe₂O were found to be constant in the studied concentration range of MnO and Fe₂O. The former increased with an increase in the CaO content, while the latter increased with an increase in the SiO₂ content.

I. INTRODUCTION

THE minimization of basic oxygen furnace (BOF) slag carried over to the ladle and the reduction of the amount of oxides (Fe₂O + MnO) that are reducible by the addition of reducing agent (Al ash, CaC₂) are very important for desulfurization, deoxidation, and inclusion control in a ladle metallurgical process. The data on the activities of Fe₂O and MnO in CaO-SiO₂-Al₂O₃-MgO slags as functions of slag composition and temperature are the most indispensable of the thermodynamic analysis for these refining processes. In previous work,¹¹ the activity coefficients of Fe₂O, $\gamma_{\text{Fe}_2\text{O}}$, in CaO-SiO₂-Al₂O₃-Fe₂O (<5 mass pct) slags were obtained at 1873 K by using a slag-metal equilibration technique. As a result, the $\gamma_{\text{Fe}_2\text{O}}$ values increased with an increase in the content of SiO₂. However, this slag composition dependence is inconsistent with previous results^{12,31} for the activity coefficients of MnO, γ_{MnO} , in the same slag system, obtained at 1923 K in a gas-slag equilibrium experiment; that is, the γ_{MnO} values increase with an increase in the content of CaO.

In this study, the activity coefficients of MnO in CaO-Al₂O₃, CaO-SiO₂, and CaO-SiO₂-Al₂O₃ slags saturated with an Al₂O₃ or CaO crucible were determined at 1873 K in a slag-metal equilibrium experiment, coupled with the activities of Al₂O₃¹⁴ in CaO-Al₂O₃ and CaO-SiO₂-Al₂O₃ slags and those of SiO₂^{14,51} in CaO-SiO₂ and CaO-SiO₂-Al₂O₃ slags or the analyzed contents of oxygen. Furthermore, the activity coefficients of Fe₂O were evaluated.

II. EXPERIMENTAL

A. Procedure

The master slags were prepared by premelting the mixture of reagent grade CaCO₃, Al₂O₃, SiO₂, and MnO in a platinum crucible. A vertical resistance furnace with heating bars of LaCrO₃ was used. The equilibrium with respect to manganese was approached from the metal or slag side in the following experiments. High-purity electrolytic iron (30 g) starting with approximately 500

to 1000 ppm oxygen and CaO-Al₂O₃-SiO₂-MnO (<10 mass pct) slag (7 g) were melted at 1873 K under a deoxidized Ar atmosphere with an appropriate amount of an Fe-1 mass pct Al, Fe-1 to 10 mass pct Si, or Fe-20 mass pct Mn alloys added by dropping afterward. Thereafter, the melts were stirred over a period of 2 to 3 hours by an Al₂O₃ rod for 90 seconds at 30-minute intervals in an Al₂O₃ crucible experiment. In a CaO crucible experiment, only two times of stirring by an Al₂O₃ rod was made for 30 seconds at 30-minute intervals in the melting period of 90 minutes in order to eliminate the influence of an Al₂O₃ stirring rod in a slag-metal equilibrium. To eliminate oxide inclusion by flotation, melts were unstirred for at least 1 hour before quenching. After equilibration, the crucible was pulled out of the furnace and quenched rapidly in a He gas stream, followed by water quenching.

B. Chemical Analysis

Detailed descriptions of the chemical analyses for acid-soluble and acid-insoluble Al,¹⁶ Si,¹⁷ Mn,¹⁸ and total oxygen¹⁹ in the metal phase and those for Al,¹⁶ Ca,^{16,71} Si,^{16,71} Mn,¹⁸ total Fe,¹¹ and metallic Fe¹¹ in the slag phase are already cited in previous articles. The manganese contents in metal and slag are also determined by inductively coupled plasma emission spectrometry after dissolution of samples using aqua regia. The results are in good agreement with those obtained by the sodium periodate oxidation absorptiometry, which was used in previous work.¹⁸

The analytical errors in the metal phase were estimated as follows:

| | |
|--------------------|------------------|
| acid-soluble Al: | ±1.5 pct (RSD); |
| acid-insoluble Al: | ±0.1 mass ppm; |
| Si: | ±1.4 pct (RSD); |
| Mn: | ±1.0 pct (RSD); |
| total O: | 1 ± 0.7 mass ppm |

Those in the slag phase were estimated as follows:

| | | | |
|-----|----------------|-----|-----------------|
| Al: | ±0.1 mass pct; | Ca: | ±0.1 mass pct; |
| Si: | ±0.1 mass pct; | Mn: | ±1.0 pct (RSD); |
| Fe: | ±1.0 pct (RSD) | | |

where RSD denotes the relative standard deviation.

HIROKI OHTA, Graduate Student, Department of Metallurgy, and HIDEAKI SUITO, Professor, Institute for Advanced Materials Processing, are with Tohoku University, Sendai 980, Japan.

Manuscript submitted July 6, 1994.

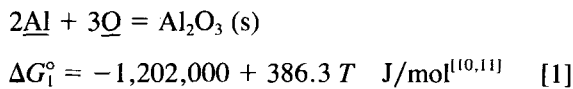
III. RESULTS AND DISCUSSION

The chemical compositions of metal and slag phases are given in Table I, and the slag compositions denoted by AC, CA, CS, CAS, and ACS are plotted in the CaO-SiO₂-Al₂O₃ phase diagram in Figure 1.

A. Aluminum-Oxygen Equilibrium

The relationships between total oxygen and total Al contents in equilibrium with CaO-Al₂O₃ slags are shown in logarithmic form in Figure 2 on mass percent base. It was experimentally confirmed in the previous studies^[6] that the total Al, which is the sum of the acid-soluble and acid-insoluble Al, corresponds to the dissolved Al at 1873 K. Thus, the contents of acid-insoluble Al given in Table I correspond to the precipitated Al₂O₃ during solidification.

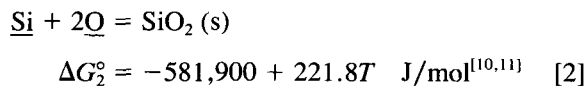
Aluminum deoxidation equilibrium can be expressed as follows:



The solid lines in Figure 2 correspond to the results calculated by the iterative method, using Rein and Chipman's values^[4] for the activities of Al₂O₃ (0.33 for AC and 0.0048 for CA) with respect to the solid standard state given in Table II, the ΔG_1° value, and the respective interaction parameters given in Table III. In the derivation of these lines, the terms related to the interaction parameters e_{O}^{Mn} and $e_{\text{Al}}^{\text{Mn}}$ were not considered. It can be seen from Figure 2 that the results for AC and CA slags follow closely the calculated lines. This finding suggests that aluminum-oxygen equilibrium in liquid iron is established, and the reported values for $a_{\text{Al}_2\text{O}_3}$ in CaO-Al₂O₃ slags are valid. Furthermore, the effect of MnO on activity of Al₂O₃ is negligibly small in the studied concentration range of MnO.

Total oxygen contents are plotted against silicon contents in logarithmic form for the CaO-SiO₂-Al₂O₃ slags (ACS-2, 4, 5) saturated with an Al₂O₃ crucible in Figure 3. Similar plots for CaO-SiO₂-Al₂O₃ (CAS-5, 8 to 11) and CaO-SiO₂ slags (CS) saturated with a CaO crucible are shown in Figure 4.

Silicon deoxidation equilibrium can be written as follows:

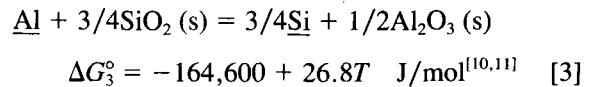


The lines in Figures 3 and 4 were calculated by the iterative method, using the a_{SiO_2} values given in Table II, the ΔG_2° value, and the respective interaction parameters given in Table III. In this calculation, the terms related to the interaction parameters e_{O}^{Mn} and $e_{\text{Si}}^{\text{Mn}}$ were not taken into account. Although the ACS, CAS, and CS slags contain MnO at the maximum levels of 9.6, 1.9, and 7.2 mass pct, respectively, as given in Table I, the data points, except for CS slag, fall easily on the thermodynamically calculated lines. This implies that the effect of MnO on the values of a_{SiO_2} is found to be negligibly small, and the values of a_{SiO_2} in CaO-SiO₂-Al₂O₃ slags given in Table II are well estimated.

The disagreement between the observed and calculated results for CS slag shown in Figure 4 may be due to the value of a_{SiO_2} (=0.068) given in Table II. The a_{SiO_2} value calculated from the present results was found to be 0.017, which is significantly smaller than the aforementioned value. Analogously, the relationship between total oxygen and total Al contents for the CaO-SiO₂-Al₂O₃ slags were plotted and compared with the calculated ones, by using the $a_{\text{Al}_2\text{O}_3}$ values given in Table II. Subsequently, a good agreement was also observed, thus suggesting that the $a_{\text{Al}_2\text{O}_3}$ values in Table II are reasonably well estimated.

B. Silicon-Aluminum Equilibrium

The exchange reaction with respect to Al and Si between slag and metal is expressed as follows:



The following relation is obtained by using the equilibrium constant of Eq. [3], K_3 :

$$\log [\text{pct Al}] = (3/4) \log [\text{pct Si}] + \log (f_{\text{Si}}^{3/4}/f_{\text{Al}})$$

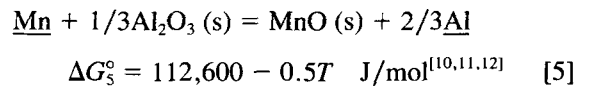
$$+ \log \{a_{\text{Al}_2\text{O}_3}^{1/2}/(K_3 \cdot a_{\text{SiO}_2}^{3/4})\} \quad [4]$$

where a_i and f_j are the activity of component i in slag with respect to solid standard state and the activity coefficient of element j in metal in Henry's state referred to one mass pct.

Total Al contents are plotted against Si contents in logarithmic form for ACS and CAS slags in Figures 5 and 6, respectively. The lines in Figures 5 and 6 were obtained from Eq. [4] by the iterative method, using the $a_{\text{Al}_2\text{O}_3}$ and a_{SiO_2} values given in Table II and the respective interaction parameters given in Table III. The data points follow closely the calculated lines, whose slopes are almost 3/4, as predicted from Eq. [4]. This indicated that the $f_{\text{Si}}^{3/4}/f_{\text{Al}}$ ratios in the second term on the right-hand side of Eq. [4] are regarded as nearly constant.

C. Manganese Distribution Ratio

The exchange reaction with respect to Mn and Al between slag and metal is expressed as



The manganese distribution ratio, L_{Mn} (= (mass pct Mn)/(mass pct Mn)), can be written, by using the equilibrium constant of Eq. [5], K_5 , as follows:

$$\log L_{\text{Mn}} = (-2/3) \log [\text{pct Al}] - \log \gamma_{\text{MnO}}$$

$$+ \log (\alpha \cdot K_5 \cdot a_{\text{Al}_2\text{O}_3}^{1/3} \cdot f_{\text{Mn}}/f_{\text{Al}}^{2/3}) \quad [6]$$

where α is the constant relating to the conversion from mole fraction of MnO to mass percent. Although α is a function of slag composition, it is regarded as approximately constant under the present experimental conditions. The term γ_{MnO} is the activity coefficient of MnO with respect to solid standard state.

The values for L_{Mn} are plotted against Al contents in

Table I. Chemical Compositions of Metal and Slag Phases

| Initial MnO (Pct) | Metal | | | | | Slag | | | | |
|-------------------|---------|-----------------|------------|------------|-----------|-----------------------------------|---------------------|-------------|--------|-----------------------------------|
| | [Al] | | [Si] (Pct) | [Mn] (Pct) | [O] (Ppm) | (Al ₂ O ₃) | (SiO ₂) | (CaO) (Pct) | (MnO) | (Fe ₂ O ₃) |
| | Soluble | Insoluble (Ppm) | | | | | | | | |
| | | | | | AC | | | | | |
| 2 | 14.3 | 2.8 | — | 0.740 | 22.1 | 64.8 | — | 33.0 | 2.22 | 0.989 |
| 2 | 9.1 | 2.0 | — | 0.600 | 23.0 | 65.1 | — | 32.7 | 2.03 | 1.03 |
| 2 | 7.0 | 1.0 | — | 0.454 | 23.0 | 64.3 | — | 33.4 | 1.48 | 1.03 |
| 2 | 1180 | 1.1 | — | 1.60 | 2.8 | 65.4 | — | 34.0 | 0.160 | 0.0381 |
| 2 | 6320 | 1.6 | — | 1.06 | 18.1 | 65.8 | — | 34.1 | 0.0408 | 0.0346 |
| 0 | 3.1 | 0.4 | — | 0.296 | 40.4 | 65.4 | — | 32.4 | 1.54 | 0.807 |
| 0 | 10.0 | 1.9 | — | 0.605 | 25.8 | 64.7 | — | 33.5 | 1.43 | 0.841 |
| 0 | 28.0 | 2.1 | — | 0.605 | 15.6 | 65.2 | — | 33.6 | 1.05 | 0.461 |
| 0 | 256 | 1.9 | — | 0.746 | 4.3 | 64.6 | — | 34.9 | 0.306 | 0.190 |
| | | | | | CA | | | | | |
| 0 | 0.7 | 0.9 | — | 1.32 | 21.4 | 42.0 | — | 56.6 | 1.37 | 2.33 |
| 0 | 0.8 | 0.8 | — | 1.42 | 19.2 | 41.8 | — | 56.7 | 1.12 | 2.17 |
| 0 | 4.0 | 0.8 | — | 1.46 | 8.9 | 42.6 | — | 56.3 | 0.505 | 1.84 |
| 0 | 53.9 | 1.0 | — | 1.54 | 1.6 | 41.9 | — | 57.8 | 0.108 | 0.588 |
| 0 | 105 | 1.7 | — | 1.62 | 1.5 | 42.5 | — | 57.4 | 0.0762 | 0.219 |
| | | | | | CS | | | | | |
| 8 | — | — | 0.0116 | 0.485 | 56.4 | — | 40.6 | 50.9 | 7.15 | 1.70 |
| 8 | — | — | 0.0044 | 0.372 | 52.4 | — | 40.9 | 51.0 | 7.10 | 1.41 |
| 8 | — | — | 0.0254 | 0.616 | 36.2 | — | 41.3 | 52.2 | 5.94 | 0.935 |
| 0 | — | — | 0.0340 | 0.106 | 27.0 | — | 43.3 | 54.5 | 0.944 | 0.740 |
| 0 | — | — | 0.0690 | 0.201 | 27.8 | — | 43.3 | 55.1 | 1.22 | 0.482 |
| 0 | — | — | 0.0746 | 0.338 | 33.4 | — | 43.1 | 53.3 | 2.56 | 0.339 |
| 0 | — | — | 0.0711 | 0.107 | 27.9 | — | 43.3 | 55.1 | 0.686 | 0.761 |
| 0 | — | — | 0.126 | 0.197 | 12.2 | — | 43.3 | 54.4 | 0.723 | 0.398 |
| | | | | | ACS-2 | | | | | |
| 10 | 1.1 | 1.0 | 0.0155 | 0.266 | 97.8 | 49.1 | 21.0 | 18.0 | 9.56 | 2.45 |
| 10 | 2.5 | 1.4 | 0.0576 | 0.426 | 77.4 | 49.8 | 21.7 | 18.7 | 8.55 | 1.37 |
| 10 | 9.5 | 1.5 | 0.200 | 0.794 | 35.5 | 48.9 | 22.7 | 18.9 | 7.67 | 0.675 |
| 10 | 2.6 | 1.5 | 0.0556 | 0.518 | 58.5 | 48.6 | 21.8 | 18.8 | 8.79 | 1.53 |
| 0 | 1.5 | 2.7 | 0.0843 | 0.0589 | 43.7 | 52.1 | 23.4 | 22.5 | 0.944 | 1.22 |
| 0 | 48.0 | 1.6 | 1.31 | 0.463 | 15.5 | 53.0 | 22.2 | 21.9 | 1.60 | 0.311 |
| | | | | | ACS-4 | | | | | |
| 5 | 14.9 | 1.2 | 0.0714 | 0.687 | 24.5 | 53.4 | 15.3 | 26.7 | 3.17 | 0.579 |
| 5 | 53.0 | 0.9 | 0.325 | 0.897 | 12.0 | 53.4 | 16.2 | 27.0 | 1.81 | 0.328 |
| 0 | 14.1 | 0.5 | 0.0553 | 0.202 | 22.3 | 53.3 | 16.1 | 30.1 | 1.03 | 0.763 |
| 0 | 12.1 | 1.0 | 0.0460 | 0.169 | 25.8 | 53.5 | 16.1 | 29.4 | 0.893 | 0.857 |
| 0 | 46.0 | 1.6 | 0.295 | 0.172 | 12.1 | 53.3 | 16.3 | 30.0 | 0.425 | 0.314 |
| | | | | | ACS-5 | | | | | |
| 2 | 1.8 | 1.4 | 0.157 | 0.0929 | 79.6 | 43.0 | 30.2 | 25.3 | 2.71 | 1.17 |
| 0 | 6.1 | 1.3 | 0.387 | 0.127 | 43.0 | 43.3 | 30.4 | 25.9 | 2.23 | 0.666 |
| 1 | 12.3 | 2.7 | 0.741 | 0.0897 | 39.5 | 43.3 | 30.2 | 25.5 | 1.25 | 0.529 |
| 0 | 10.8 | 8.4 | 1.24 | 0.0938 | 35.3 | 44.3 | 29.4 | 24.9 | 0.939 | 0.409 |
| 0.5 | 28.9 | 4.3 | 2.11 | 0.0511 | 28.9 | 42.7 | 31.0 | 26.0 | 0.377 | 0.241 |
| | | | | | CAS-5 | | | | | |
| 3 | 0.1 | 2.4 | 0.0007 | 0.759 | 19.8 | 28.5 | 18.0 | 51.9 | 1.88 | 0.700 |
| 0 | 37.2 | 1.8 | 0.0583 | 0.879 | 5.9 | 28.1 | 18.0 | 53.1 | 0.232 | 0.138 |
| 3 | 25.7 | 3.0 | 0.0339 | 0.849 | 5.7 | 28.3 | 16.4 | 54.2 | 0.319 | 0.264 |
| 0 | 136 | 2.1 | 0.283 | 1.64 | 3.2 | 30.6 | 16.6 | 52.0 | 0.200 | 0.0725 |
| 3 | 369 | 3.8 | 1.15 | 1.44 | 1.6 | 28.8 | 18.1 | 53.4 | 0.0950 | 0.0329 |
| | | | | | CAS-8 | | | | | |
| 0 | 3.2 | 1.4 | 0.0016 | 1.39 | 6.5 | 29.8 | 10.0 | 59.8 | 0.439 | 0.302 |
| 0 | 14.4 | 1.2 | 0.0168 | 1.63 | 2.7 | 29.3 | 9.81 | 61.3 | 0.175 | 0.142 |
| 0 | 13.0 | 1.3 | 0.0238 | 1.26 | 3.3 | 29.2 | 9.84 | 59.8 | 0.126 | 0.133 |
| 0 | 49.0 | 0.4 | 0.0647 | 1.67 | 1.7 | 29.6 | 9.25 | 60.1 | 0.0812 | 0.0737 |
| 0 | 108 | 2.1 | 0.248 | 1.39 | 1.0 | 30.1 | 9.66 | 60.1 | 0.0370 | 0.0488 |
| | | | | | CAS-9 | | | | | |
| 1.5 | 1.8 | 0.4 | 0.0160 | 0.529 | 37.6 | 24.0 | 24.8 | 49.6 | 1.25 | 0.621 |
| 0 | 15.9 | 1.2 | 0.147 | 0.447 | 11.0 | 23.7 | 25.6 | 49.8 | 0.366 | 0.234 |
| 3 | 87.2 | 5.5 | 0.988 | 0.820 | 5.2 | 22.3 | 25.2 | 51.0 | 0.207 | 0.0919 |
| | | | | | CAS-10 | | | | | |
| 2 | 2.6 | 1.1 | 0.0770 | 0.511 | 28.1 | 15.1 | 32.5 | 50.6 | 1.08 | 0.515 |
| 0 | 5.4 | 2.1 | 0.172 | 0.543 | 13.9 | 14.8 | 33.3 | 50.5 | 0.785 | 0.298 |
| 1.5 | 10.7 | 3.2 | 0.340 | 0.449 | 15.2 | 16.0 | 32.9 | 49.9 | 0.495 | 0.232 |
| 0 | 19.7 | 4.5 | 0.813 | 0.410 | 11.9 | 16.0 | 33.5 | 49.0 | 0.283 | 0.201 |
| 1.5 | 20.6 | 4.9 | 1.17 | 0.501 | 12.5 | 15.0 | 33.0 | 50.5 | 0.322 | 0.112 |
| | | | | | CAS-11 | | | | | |
| 0 | 9.9 | 0.9 | 0.0359 | 0.760 | 10.7 | 29.0 | 20.4 | 50.3 | 0.514 | 0.250 |
| 0 | 18.1 | 1.2 | 0.0608 | 0.964 | 9.7 | 28.7 | 21.0 | 49.9 | 0.585 | 0.202 |
| 0 | 44.0 | 1.2 | 0.185 | 1.38 | 5.9 | 28.3 | 21.0 | 49.5 | 0.546 | 0.117 |
| 0 | 62.1 | 1.3 | 0.311 | 1.40 | 5.5 | 28.5 | 21.2 | 50.2 | 0.328 | 0.104 |

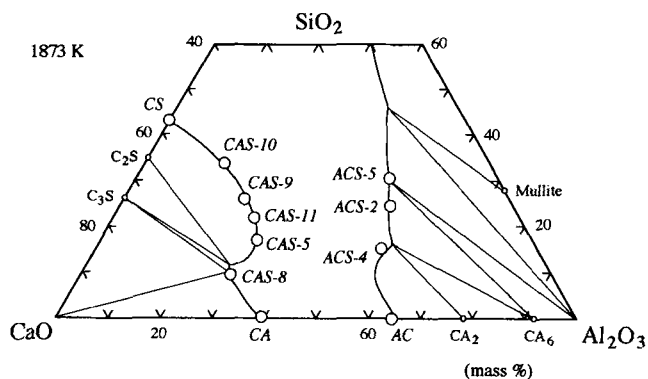


Fig. 1—Experimental slag compositions plotted in CaO-Al₂O₃-SiO₂ phase diagram.

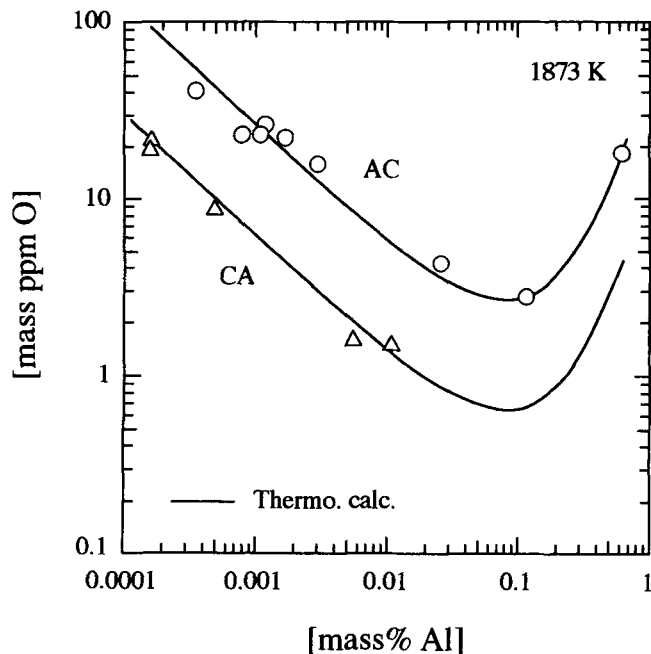


Fig. 2—Aluminum-oxygen equilibrium for CaO-Al₂O₃ slags (AC, CA).

Table II. Activities of SiO₂ and Al₂O₃ at 1873 K^[4]

| Slag | a_{SiO_2} | $a_{\text{Al}_2\text{O}_3}$ |
|--------|----------------------|-----------------------------|
| AC | — | 0.33 |
| CA | — | 0.0048 |
| CS | 0.068 ^[7] | — |
| CAS-2 | 0.11 | 0.81 |
| ACS-4 | 0.015 | 0.60 |
| ACS-5 | 0.33 | 1 |
| CAS-5 | 0.00063 | 0.063 |
| CAS-8 | 0.000077 | 0.0021 ^[11] |
| CAS-9 | 0.0068 | 0.066 |
| CAS-10 | 0.020 | 0.056 |
| CAS-11 | 0.0020 | 0.072 |

logarithmic form in Figure 7 for AC and CA slags. The finding that the experimental points follow the straight lines with a slope of $-2/3$, as expected from Eq. [6], indicates that the second and third terms on the right-hand side of Eq. [6] are constant.

Table III. Interaction Parameters at 1873 K Used in the Present Work^[11]

| i | j | $e_i^j (r_i^j)$ |
|-----|-----|-----------------|
| Al | Al | 0.045 (-0.001) |
| | Si | 0.056 |
| | O | -6.6 |
| Si | Al | 0.058 |
| | Si | 0.11 (-0.0021) |
| | O | -0.23 |
| | Mn | 0.002 |
| O | Al | -3.9 (1.7) |
| | Si | -0.131 |
| | O | -0.20 |
| | Mn | -0.021 |
| Mn | Si | 0 |
| | O | -0.083 |
| | Mn | 0 |

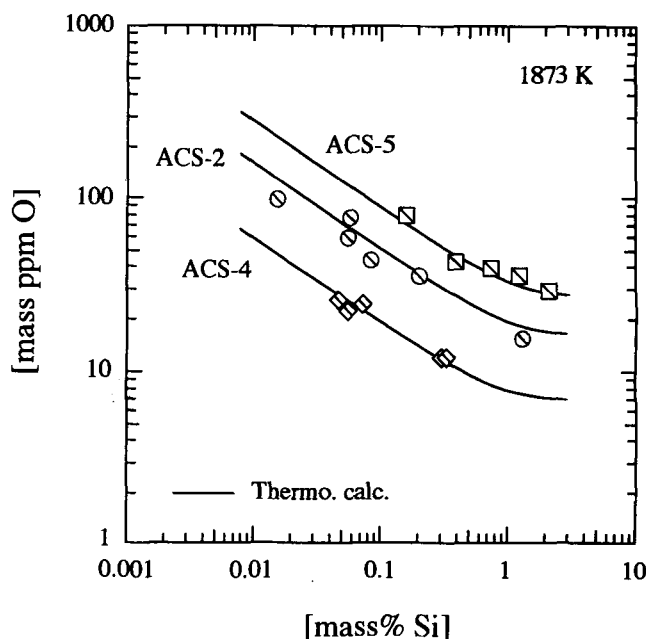
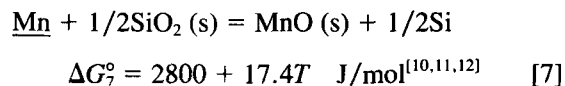


Fig. 3—Silicon-oxygen equilibrium for CaO-Al₂O₃-SiO₂ slags (ACS-2, 4, 5).

Slag/metal reaction with respect to Mn and Si can be expressed as follows:



The following relation can be deduced from Eq. [7]:

$$\log L_{\text{Mn}} = (-1/2) \log [\text{pct Si}] - \log \gamma_{\text{MnO}}$$

$$+ \log (\beta \cdot K_7 \cdot a_{\text{SiO}_2}^{1/2} \cdot f_{\text{Mn}}/f_{\text{Si}}^{1/2}) \quad [8]$$

where K_7 is the equilibrium constant of Eq. [7] and β is the same meaning as α in Eq. [6].

The relationships between $\log L_{\text{Mn}}$ and $\log [\text{pct Si}]$ for ACS-2, 4, 5 slags, CAS-5, 8, 11 slags, and CAS-9, 10, and CS slags are shown in Figures 8, 9, and 10, respectively. It can be seen that all data points fall easily

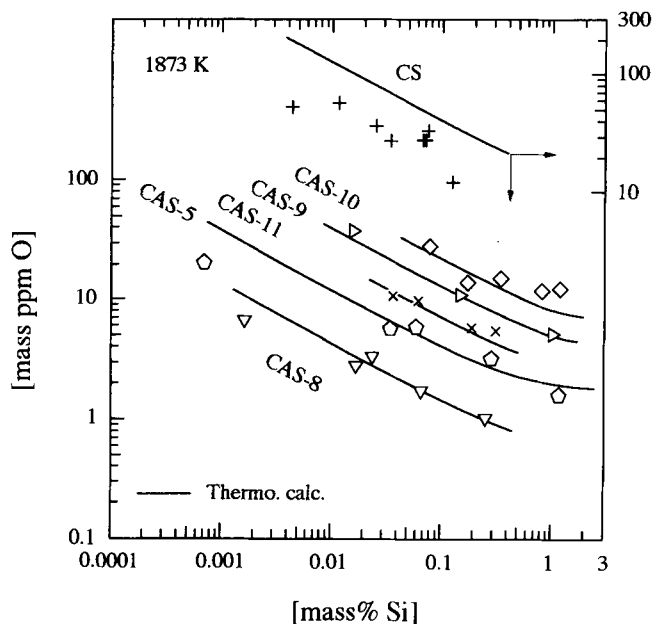
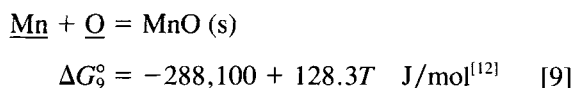


Fig. 4—Silicon-oxygen equilibrium for CaO-SiO₂ (CS) and CaO-Al₂O₃-SiO₂ slags (CAS-5, 8 to 11).

on the lines with a slope of $-1/2$, as predicted from Eq. [8]. This implies that the $a_{\text{SiO}_2}^{1/2}/\gamma_{\text{MnO}}$ ratios are independent of the MnO content in the respective slags under a dilute solution range of metal phase. Furthermore, the highest value of L_{Mn} at a given Si level was obtained for ACS slag. A plot of $\log L_{\text{Mn}}$ vs $\log [\text{pct Al}]$ for CaO-SiO₂-Al₂O₃ slags also showed a good linear relationship, as is obvious from the relations between $\log [\text{pct Al}]$ and $\log [\text{pct Si}]$ which is indicated in Figure 6.

D. Activity Coefficient of MnO

Manganese deoxidation equilibrium can be expressed as follows:



Using the equilibrium constant for Reaction [9], K_9 , we have the following relation:

$$\log \gamma_{\text{MnO}} = \log ([\text{pct Mn}] \cdot [\text{pct O}]/X_{\text{MnO}}) + \log (K_9 \cdot f_{\text{Mn}} \cdot f_{\text{O}}) \quad [10]$$

where X_{MnO} is the mole fraction of MnO.

The values for γ_{MnO} with respect to solid standard state can be obtained from Eq. [10] by using the experimental results given in Table I and the respective interaction parameters given in Table III. These results for AC, CA, ACS, CAS, and CS slags are plotted against mole fraction of MnO in Figures 11 through 14 by open marks. The γ_{MnO} values can also be estimated from Eq. [6] by using the $a_{\text{Al}_2\text{O}_3}$ values given in Table II. The results for AC, CA, ACS, and CAS slags are shown by the marks with bar in Figures 11 through 14. Similarly, the γ_{MnO} values calculated from Eq. [8] by using the a_{SiO_2} values given in Table II are shown in Figures 12 through 14 by

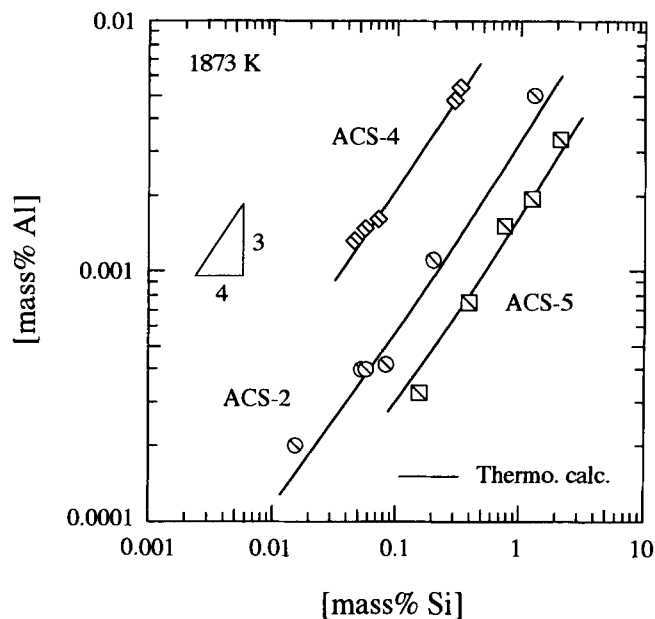


Fig. 5—Relation between aluminum and silicon contents for CaO-Al₂O₃-SiO₂ slags (ACS-2, 4, 5).

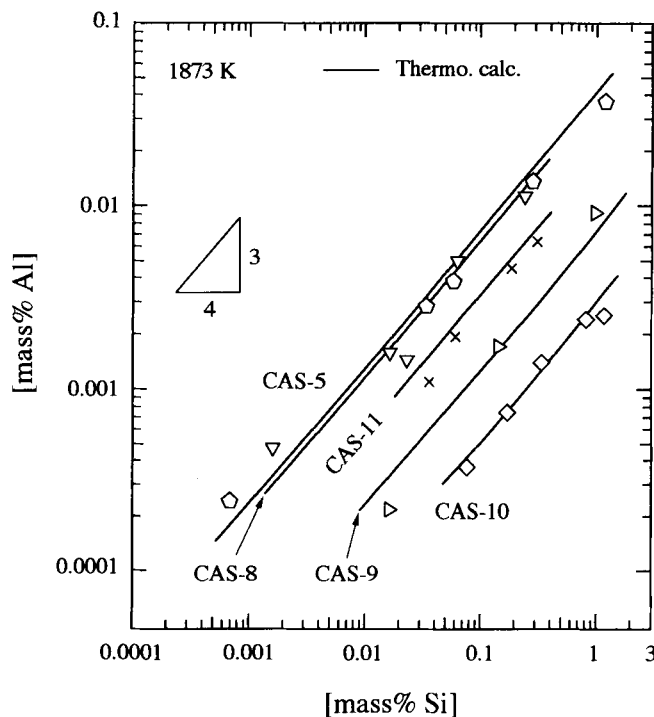


Fig. 6—Relation between aluminum and silicon contents for CaO-Al₂O₃-SiO₂ slags (CAS-5, 8 to 11).

the half-filled marks. It follows, thus, that the γ_{MnO} values calculated from three different methods, which are summarized in Table IV, are independent of mole fraction of MnO in the studied concentration range of MnO. These values are in agreement with each other, except for the values for the CS slag shown in Figure 14, although the data, particularly those for CAS slag, scatter to considerable degree.

The average values for γ_{MnO} given in Table IV are

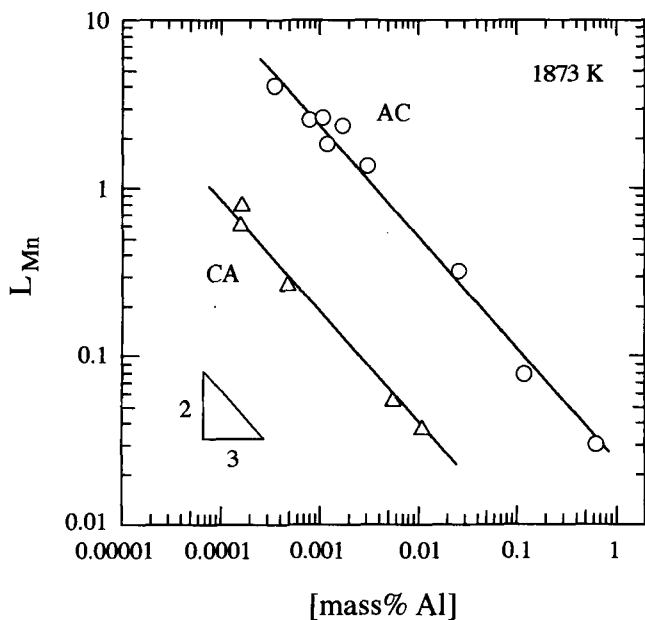


Fig. 7—Manganese distribution ratio, L_{Mn} , plotted against aluminum content for CaO-Al₂O₃ slags (AC, CA).

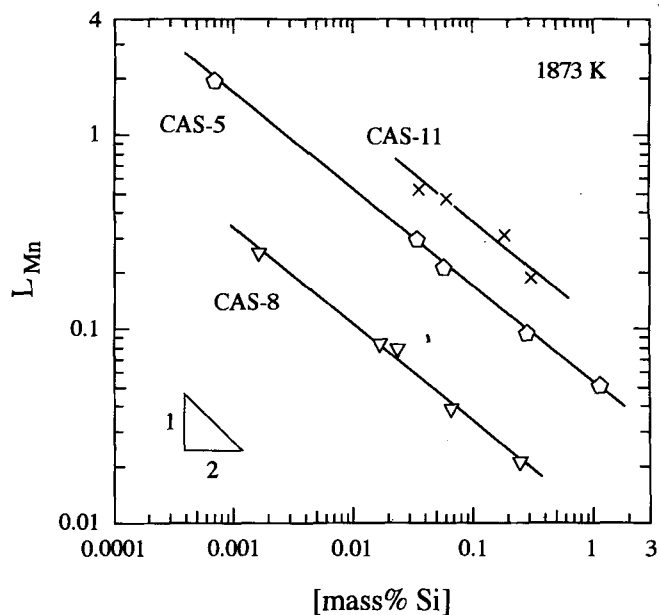


Fig. 9—Manganese distribution ratio, L_{Mn} , plotted against silicon content for CaO-Al₂O₃-SiO₂ slags (CAS-5, 8, 11).

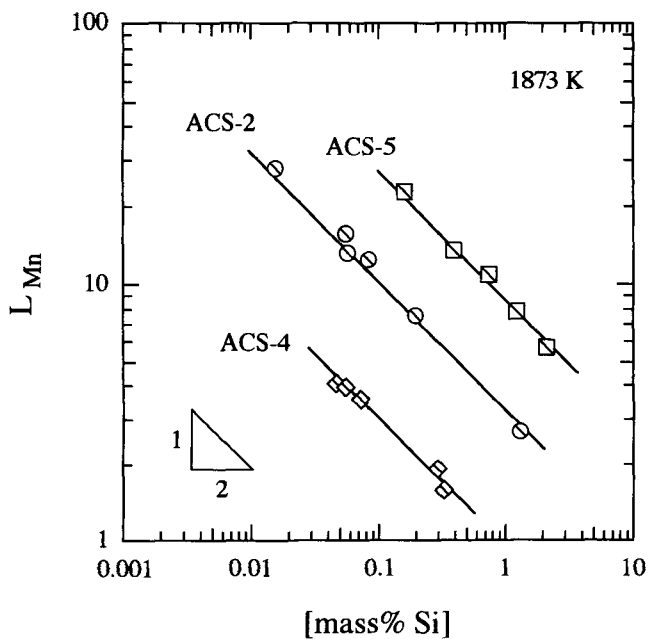


Fig. 8—Manganese distribution ratio, L_{Mn} , plotted against silicon content for CaO-Al₂O₃-SiO₂ slags (ACS-2, 4, 5).

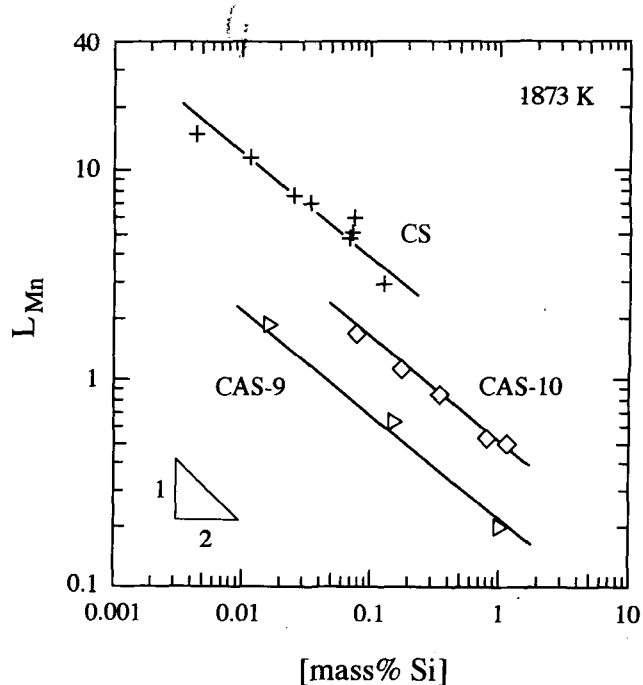


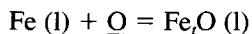
Fig. 10—Manganese distribution ratio, L_{Mn} , plotted against silicon content for CaO-SiO₂ (CS) and CaO-Al₂O₃-SiO₂ slags (CAS-9, 10).

plotted in the CaO-SiO₂-Al₂O₃ ternary diagram in Figure 15. In the case of the γ_{MnO} value for CS slag, the value calculated from Eq. [10] was used and the γ_{MnO} value was found to be 0.94. On the other hand, if the a_{SiO_2} value for CS slag obtained by Inoue and Suito^[7] was used for the calculation of γ_{MnO} from Eq. [8], the γ_{MnO} value was obtained as 2.0. The iso- γ_{MnO} lines indicated by broken lines were drawn, assuming that the present results follow the same slag composition dependence as observed at 1923 K by Abraham *et al.*^[2] and Mehta and Richardson.^[3] The γ_{MnO} values increase with increasing the content of CaO and tend to be maximum at the slag

composition of the highest solubility of CaO. The present γ_{MnO} values obtained at 1873 K are roughly two times greater than those obtained at 1923 K.^[2,3]

E. Activity Coefficient of Fe₂O

Activity coefficients of Fe₂O were estimated from the analyzed values of oxygen by using the following reaction:



$$\Delta G_{11}^{\circ} = -116,100 + 48.79T \text{ J/mol}^{[13]} \quad [11]$$

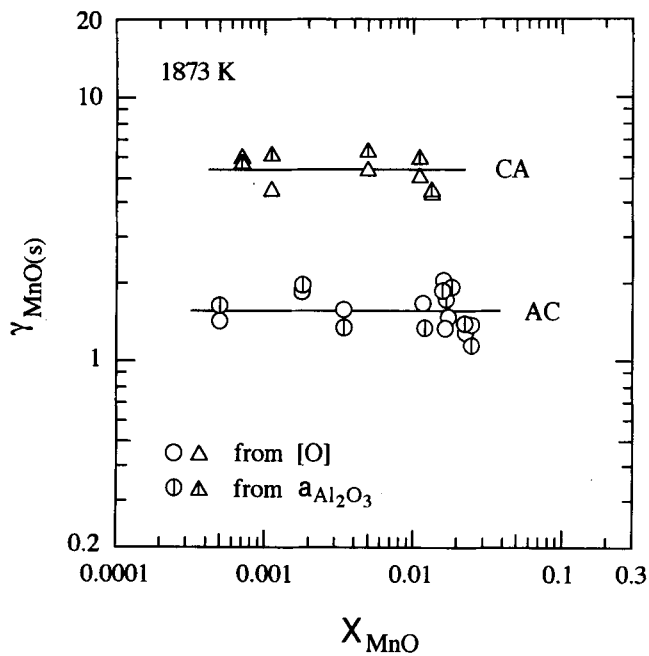
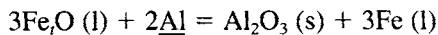


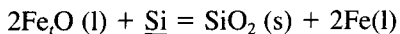
Fig. 11—Activity coefficient of MnO for CaO-Al₂O₃ slags (AC, CA).

The results are given in Table V. In a manner similar to the derivation of γ_{MnO} , as explained in Section D, the $\gamma_{\text{Fe}_2\text{O}}$ values were obtained from the following Eqs. [12] and [13], by using the values for $a_{\text{Al}_2\text{O}_3}$ and a_{SiO_2} given in Table II:



$$\Delta G_{12}^\circ = -853,900 + 239.97T \text{ J/mol}^{[10,11,13]} \quad [12]$$

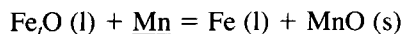
The reaction of Fe₂O with Si can be written as



$$\Delta G_{13}^\circ = -349,700 + 124.27T \text{ J/mol}^{[10,11,13]} \quad [13]$$

The $\gamma_{\text{Fe}_2\text{O}}$ values calculated from Eqs. [12] and [13] are also listed in Table V. As mentioned previously, the Fe₂O value for CS slag calculated from Eq. [13] is significantly different from that calculated from Eq. [11]. It was observed, however, that the $\gamma_{\text{Fe}_2\text{O}}$ values for other slags obtained by the above-mentioned three methods agreed reasonably well with each other.

The $\gamma_{\text{Fe}_2\text{O}}$ value can also be estimated from Eq. [14].



$$\Delta G_{14}^\circ = -172,000 + 79.57T \text{ J/mol}^{[12,13]} \quad [14]$$

The $\gamma_{\text{Fe}_2\text{O}}$ values calculated from the average values of γ_{MnO} listed in Table IV are given in Table V. In the case of the $\gamma_{\text{Fe}_2\text{O}}$ value for the CS slag, the γ_{MnO} value obtained by Eq. [10] was used and the $\gamma_{\text{Fe}_2\text{O}}$ value was found to be 2.5. On the other hand, if the a_{SiO_2} value for the CS slag obtained by Inoue and Suito^[7] was used for the calculation of $\gamma_{\text{Fe}_2\text{O}}$ from Eq. [13], the $\gamma_{\text{Fe}_2\text{O}}$ value was obtained as 5.5. The $\gamma_{\text{Fe}_2\text{O}}$ values calculated from Eqs. [11] through [14] were plotted against the mole fraction of Fe₂O. As a result, the $\gamma_{\text{Fe}_2\text{O}}$ values were observed to be independent of the mole fraction of Fe₂O in the studied

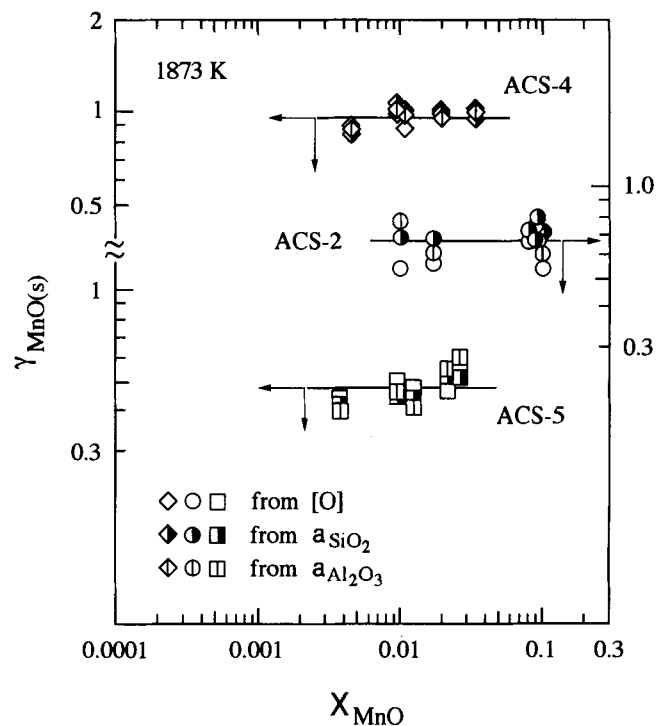


Fig. 12—Activity coefficient of MnO for CaO-Al₂O₃-SiO₂ slags (ACS-2, 4, 5).

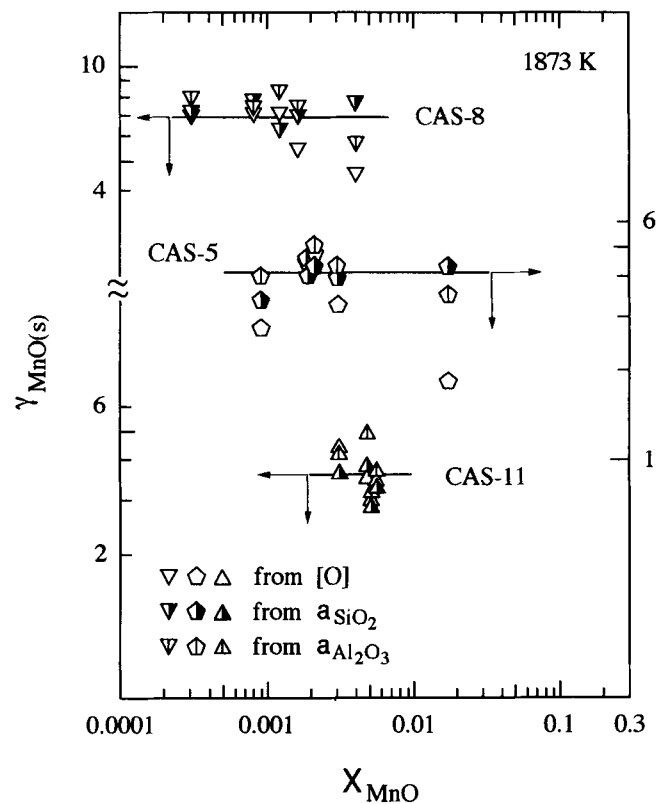


Fig. 13—Activity coefficient of MnO for CaO-Al₂O₃-SiO₂ slags (CAS-5, 8, 11).

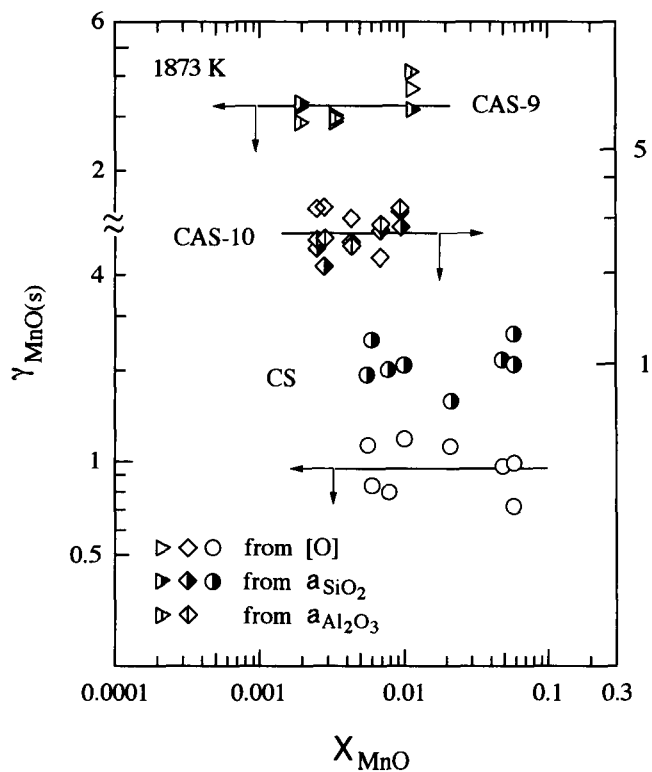


Fig. 14—Activity coefficient of MnO for CaO-SiO₂ (CS) and CaO-Al₂O₃-SiO₂ slags (CAS-9, 10).

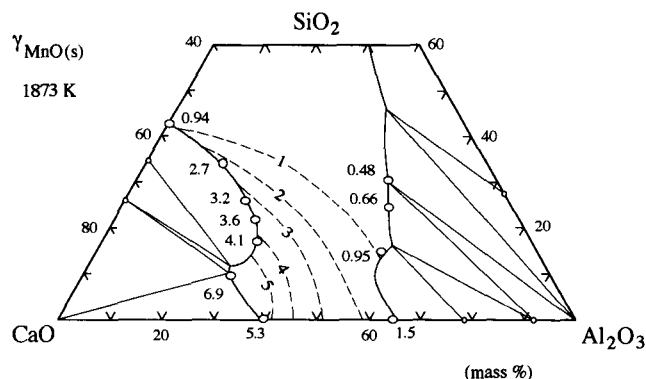


Fig. 15—Activity coefficient of MnO for CaO-Al₂O₃-SiO₂ slags.

concentration range of (mass pct Fe₂O) < 2.5. The present values for $\gamma_{\text{Fe}_2\text{O}}$ are plotted in the CaO-SiO₂-Al₂O₃ phase diagram in Figure 16, along with previous results obtained by Lee and Suito.^[1] In contrast to the results for γ_{MnO} in Figure 15, the $\gamma_{\text{Fe}_2\text{O}}$ values increase with an increase in the content of SiO₂.

IV. CONCLUSIONS

The activity coefficients of MnO and Fe₂O in the CaO-SiO₂-Al₂O₃ slags were studied at 1873 K in a slag-metal equilibrium experiment, and the following conclusions are summarized.

Table IV. Activity Coefficients of MnO

| Slag | log γ_{MnO} | | | |
|--------|---------------------------|--------------|--------------|--------------|
| | From Eq. [10] | From Eq. [8] | From Eq. [6] | Average |
| AC | 0.18 ± 0.07 | — | 0.19 ± 0.08 | 0.19 ± 0.07 |
| CA | 0.70 ± 0.06 | — | 0.76 ± 0.06 | 0.73 ± 0.06 |
| CS | -0.03 ± 0.08 | 0.31 ± 0.07 | — | — |
| ACS-2 | -0.21 ± 0.06 | -0.15 ± 0.03 | -0.17 ± 0.05 | -0.18 ± 0.05 |
| ACS-4 | -0.03 ± 0.03 | -0.02 ± 0.03 | -0.02 ± 0.02 | -0.02 ± 0.03 |
| ACS-5 | -0.31 ± 0.04 | -0.33 ± 0.04 | -0.32 ± 0.08 | -0.32 ± 0.05 |
| CAS-5 | 0.51 ± 0.17 | 0.60 ± 0.04 | 0.63 ± 0.06 | 0.58 ± 0.11 |
| CAS-8 | 0.79 ± 0.09 | 0.86 ± 0.04 | 0.87 ± 0.06 | 0.84 ± 0.07 |
| CAS-9 | 0.51 ± 0.05 | 0.49 ± 0.02 | 0.51 ± 0.09 | 0.51 ± 0.05 |
| CAS-10 | 0.46 ± 0.07 | 0.39 ± 0.05 | 0.43 ± 0.05 | 0.43 ± 0.06 |
| CAS-11 | 0.55 ± 0.07 | 0.53 ± 0.06 | 0.60 ± 0.08 | 0.56 ± 0.07 |

Table V. Activity Coefficients of Fe₂O

| Slag | log $\gamma_{\text{Fe}_2\text{O}}$ | | | |
|--------|------------------------------------|---------------|---------------|---------------|
| | From Eq. [11] | From Eq. [12] | From Eq. [13] | From Eq. [14] |
| AC | 0.00 ± 0.21 | 0.01 ± 0.23 | — | 0.01 ± 0.20 |
| CA | -0.56 ± 0.23 | -0.51 ± 0.19 | — | -0.53 ± 0.23 |
| CS | 0.40 ± 0.17 | — | 0.74 ± 0.12 | 0.40 ± 0.14 |
| ACS-2 | 0.26 ± 0.09 | 0.30 ± 0.07 | 0.32 ± 0.05 | 0.30 ± 0.06 |
| ACS-4 | 0.17 ± 0.06 | 0.18 ± 0.05 | 0.18 ± 0.04 | 0.18 ± 0.06 |
| ACS-5 | 0.47 ± 0.02 | 0.46 ± 0.07 | 0.45 ± 0.04 | 0.46 ± 0.04 |
| CAS-5 | 0.17 ± 0.11 | 0.29 ± 0.11 | 0.27 ± 0.17 | 0.24 ± 0.15 |
| CAS-8 | 0.01 ± 0.06 | 0.09 ± 0.07 | 0.08 ± 0.12 | 0.06 ± 0.10 |
| CAS-9 | 0.39 ± 0.10 | 0.39 ± 0.15 | 0.37 ± 0.06 | 0.39 ± 0.07 |
| CAS-10 | 0.48 ± 0.10 | 0.44 ± 0.09 | 0.41 ± 0.08 | 0.44 ± 0.08 |
| CAS-11 | 0.36 ± 0.02 | 0.40 ± 0.06 | 0.34 ± 0.04 | 0.37 ± 0.07 |

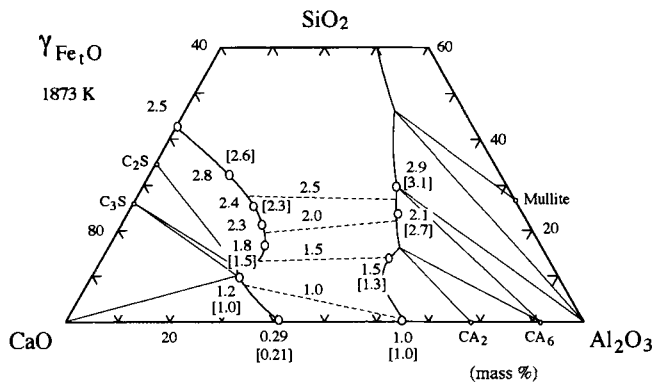


Fig. 16—Activity coefficient of Fe_2O for $\text{CaO-Al}_2\text{O}_3\text{-SiO}_2$ slags. The results in brackets are by Lee and Suito.¹¹

1. Activity coefficients of MnO obeyed Henry's law in the concentration range of (mass pct MnO) < 9.6 and increased with an increase in the content of CaO .
2. Activity coefficients of Fe_2O obeyed Henry's law in the concentration range of (mass pct Fe_2O) < 2.5 and increased with an increase in the content of SiO_2 .

REFERENCES

1. K.R. Lee and H. Suito: *Metall. Mater. Trans. B*, 1994, vol. 25B, pp. 893-902.
2. K.P. Abraham, M.W. Davies, and F.D. Richardson: *J. Iron Steel Inst.*, 1960, vol. 196, pp. 82-89.
3. S.R. Mehta and F.D. Richardson: *J. Iron Steel Inst.*, 1965, vol. 203, pp. 524-28.
4. R.H. Rein and J. Chipman: *Trans. TMS-AIME*, 1965, vol. 233, pp. 415-25.
5. S.-W. Cho and H. Suito: *Iron Steel Inst. Jpn. Int.*, 1994, vol. 34, pp. 177-85.
6. H. Suito, H. Inoue, and R. Inoue: *Iron Steel Inst. Jpn. Int.*, 1991, vol. 31, pp. 1381-88.
7. R. Inoue and H. Suito: *Metall. Trans. B*, 1992, vol. 23B, pp. 613-21.
8. H. Suito and R. Inoue: *Trans. Iron Steel Inst. Jpn. Int.*, 1984, vol. 24, pp. 257-65.
9. R. Inoue and H. Suito: *Mater. Trans. Jpn. Inst. Met.*, 1991, vol. 32, pp. 1164-69.
10. J.F. Elliott, M. Gleiser, and V. Ramakrishna: *Thermochemistry for Steelmaking*, Addison-Wesley, London, 1963, vol. 2, pp. 620-21.
11. G.K. Sigworth and J.F. Elliott: *Met. Sci.*, 1974, vol. 8, pp. 298-310.
12. H. Gaye, C. Gatellier, M. Nadif, P.V. Riboud, J. Saleil, and M. Faral: *Rev. Metall.-CIT*, 1987, Nov., pp. 759-71.
13. H. Suito and R. Inoue: *Trans. Iron Steel Inst. Jpn.*, 1984, vol. 24, pp. 301-07.